Automated Station Planning for Terrestrial Laser Scanning in Complex Forest Environments

Wenbo Zhang[1], Zhenyang Hui [1,*], Yuanping Xia[1], Penggen Cheng[1], Jialin Fu [1], Zhilu Zhang [1], Ting Hui [2]

[1] School of Surveying and Geoinformation Engineering, East China University of Technology, Nanchang, China – 2024110247@ecut.edu.cn, huizhenyang2008@163.com, ypxia@ecut.edu.cn, pgcheng@ecut.edu.cn, 2024120611@ecut.edu.cn, 2024120567@ecut.edu.cn
[2] College of Management, Guangdong AIB Polytechnic, Guangzhou, China – thui@gdaib@edu.cn

Keywords: Terrestrial laser scanner, Scan planning, Visibility analysis, Integer linear programming.

Abstract

Terrestrial laser scanning technology can efficiently acquire high-precision three-dimensional spatial information in complex forest environments, making it an important technical means for detailed analysis of forest structure and resource monitoring. However, traditional terrestrial laser scanners planning methods are prone to coverage gaps and data redundancy due to factors such as tree obstructions, terrain undulations, and canopy overlap, making it difficult to simultaneously balance observation completeness and scanner station deployment cost. To address this, this paper proposes an intelligent survey station planning for terrestrial laser scanners in complex forest environments. The method first uses UAV LiDAR data to build a prior forest model, which is then used to quantitatively evaluate forest visibility features by calculating the cumulative visible central angle through visibility analysis. Finally, an integer linear programming model is further introduced to achieve global optimization of the station set based on an initial feasible coverage solution obtained using a greedy algorithm. To test the performance of the proposed method, this paper applies the proposed method to the forest plot located in Lushan city, Jiangxi province, China. Experimental results indicate that the proposed method achieves an overall coverage rate of 94.55% with only seven stations, reducing the number of stations by approximately 30% and 22% compared with the greedy algorithm and genetic algorithm, respectively. The results demonstrate the effectiveness and superiority of this method for station planning in complex forest areas and provide efficient and precise technical support for forest structure monitoring and spatial information acquisition.

1. Introduction

As an important component of terrestrial ecosystems, forests play a crucial role in maintaining the carbon cycle balance, protecting species diversity, and sustaining climate stability (Hui et al., 2025). The forest ecosystem has a complex structure, and how to quickly and efficiently obtain forest information is of great significance for forest resource monitoring and the sustainable development of forest ecosystems (Calders et al., 2020). With the development of remote sensing technology, hyperspectral remote sensing, drone imagery, LiDAR, and other technologies are gradually being applied to forestry research (Panagiotidis et al., 2022). Terrestrial Laser Scanning (TLS) systems can efficiently and accurately acquire spatial data of large forest areas by precisely measuring ground points, making them especially suitable for complex forestry ecological environments (Liu et al., 2017). Compared with traditional manual survey methods, TLS not only improves measurement accuracy but also significantly reduces survey time[1] and labor costs (Wujanz et al., 2017). However, at present, the selection of TLS scanning positions mainly relies on the operator's experience, lacking guidance from scientific theory (Chen et al., 2022). When the observation scope expands or the observation environment changes, it is impossible to ensure that the coverage, accuracy, and level of detail of the data meet its quality requirements, resulting in data redundancy and gaps, which in turn seriously affect usage costs and work efficiency (Ahn and Wohn, 2016). Therefore, it is particularly important to develop an appropriate planning scheme before data collection and to determine the optimal TLS observation network.

The process of determining the optimal set of observation positions to achieve complete coverage and high-precision 3D reconstruction of a target scene, while satisfying constraints such as measuring range, field of view, and occlusion, is referred to as the viewpoint planning problem (VPP) (Karaszewski et al., 2016). Early studies were mostly based on two-dimensional models, determining the minimal set of viewpoints through methods such as visibility polygons (Li et al., 2021), discretized candidate viewpoints (Chen et al., 2018) or greedy algorithms (Latimer. et al., 2004). However, two-dimensional models struggle to accurately reflect the spatial

* Corresponding author

structure and occlusion relationships of real-world scenes, limiting their application in complex natural environments. ULS LiDAR and UAV photogrammetry provide high-resolution prior data for this process, enabling visibility analysis and site optimization in three-dimensional space. (Chen et al., 2022) quickly generated large-scale regional 3D models through UAV photogrammetry and point cloud processing technologies. (Noichl et al., 2024) allows for the input of any 3D model or point cloud. The input three-dimensional scene is automatically processed into a triangulated mesh and the mesh resolution is optimized through the midpoint subdivision method. In contrast, three-dimensional models can more comprehensively represent forest structure and terrain features, but they also pose challenges such as large data volumes and high computational complexity. Therefore, how to achieve a lightweight representation and efficient planning of three-dimensional models while preserving the authenticity of forest spatial characteristics has become a key challenge in the current research on optimizing forest TLS observation networks.

The planning problem for terrestrial LiDAR observation network is typically a combinatorial optimization problem, aiming to select an optimal set of observation points to achieve coverage of the target area data scanning while satisfying a series of constraints (Rebolj et al., 2017). A common method for resolving such problems is the greedy algorithm, which constructs a solution step by step based on a predetermined 'greedy criterion.' However, since it does not perform global optimization, the optimal solution obtained is only locally optimal. Regarding this issue, researchers use various methods to obtain approximately optimal solutions in order to approach the best scheme and progressively improve the greedy algorithm (Ahn and Wohn, 2016; Chen et al., 2018); Bi et al., 2022). (Chen et al., 2018) proposed a greedy algorithm with a backtracking process to mitigate the redundancy phenomenon in the results obtained by the standard greedy algorithm; (Dehbi et al., 2021) proposed an optimization method based on integer linear programming to obtain the optimal solution, and introduced flow-based constraint formulas to achieve connectivity between the selected locations. (Knechtel et al., 2022) proposed a two-stage approach based on mixed-integer linear programming (MILP) and the traveling salesman problem (TSP) to achieve efficient mobile scanning.

Although many terrestrial laser scanner planning methods have been proposed, there are still three main issues need to be solved: First, the generation of candidate scanning positions lacks spatial constraint representation, making it difficult to adequately reflect the distribution of trees and the geometric characteristics of the canopy. Second, the accuracy of visibility models is limited, making it challenging to comprehensively describe occlusion effects, field of view, and ranging constraints, which leads to uneven coverage and redundant overlap. Third, the level of intelligence in optimization algorithms is insufficient, making it difficult to balance coverage, the number of survey stations, and redundancy control under a globally optimal solution.

To solve these challenges, this paper proposes a hybrid optimization planning method that integrates heuristic search with integer linear programming. The method uses a canopy height model constructed from UAV LiDAR data as a prior and automatically generates candidate survey stations based on scanning geometry constraints. Hereafter, high-precision visibility modeling is achieved through occlusion analysis and angular interval calculations. Subsequently, the method employs a combination of heuristic filtering and ILP global optimization to minimize the number of survey stations while maximizing coverage. This approach provides a new conceptual and technical pathway for the intelligent planning of TLS observation networks in complex forested areas.

2. Methodology

This study proposes a hybrid heuristic–integer linear programming framework to optimize TLS station placement for maximum coverage with minimal stations. The flowchart of the proposed method is illustrated in Figure 1. Firstly, UAV LiDAR data is used to analyze the spatial structure of the forest and automatically generate scientifically reasonable candidate scanning positions. Next, detailed visibility analysis is conducted through geometric constraints to quantitatively assess each point's visible range and the obstruction by trees. Finally, a two-stage optimization strategy combining heuristic search and integer linear programming is employed to obtain a measurement station layout that maximizes coverage while minimizing the number of stations. To sum up, three main steps are included in this paper: 2.1 selecting the effective candidates for the TLS location, 2.2 visibility analysis based on geometric constraints, 2.3 hybrid heuristic integer linear programming algorithm.

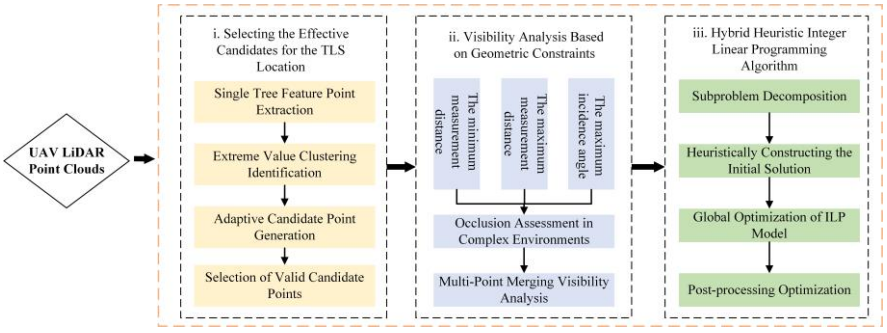

Figure 1. Flowchart of the proposed method.

This contribution has been peer-reviewed. The double-blind peer-review was conducted on the basis of the full paper.
https://doi.org/10.5194/isprs-annals-XI-1-2026-111-2026

2.1 Selecting the Effective Candidates for the TLS Location

To achieve automatic identification of individual tree crowns, spatial structure representation, and optimal terrestrial LiDAR scan station layout, this study proposes a forest spatial analysis framework based on multi-source geometric constraints. First, the UAV LiDAR point cloud is projected onto a regular grid space, and the highest point within each cell is selected to construct the canopy surface elevation. Noise suppression and structural continuity enhancement are achieved through Gaussian smoothing and interpolation operators, thereby ensuring the geometric stability of the canopy surface. On this basis, individual tree apices were identified using a local maxima detection approach, in which the analysis window size was adaptively adjusted according to forest structural conditions to avoid scale mismatch caused by fixed window settings in complex forest environments, thereby enabling the extraction of the spatial distribution of individual tree tops. To prevent field-of-view occlusion caused by TLS scanning positions being located too close to tree stems, a safety buffer strategy was introduced to define dynamic non-overlapping areas. Specifically, each individual tree was assigned a buffer zone centered at the tree stem, with a radius set to 1.5 times the stem radius. Grid nodes falling within these buffer zones were automatically excluded through point-wise filtering, and only nodes located in open areas and satisfying the requirements for instrument setup were retained as candidate scanning positions, as shown in Figure 2.

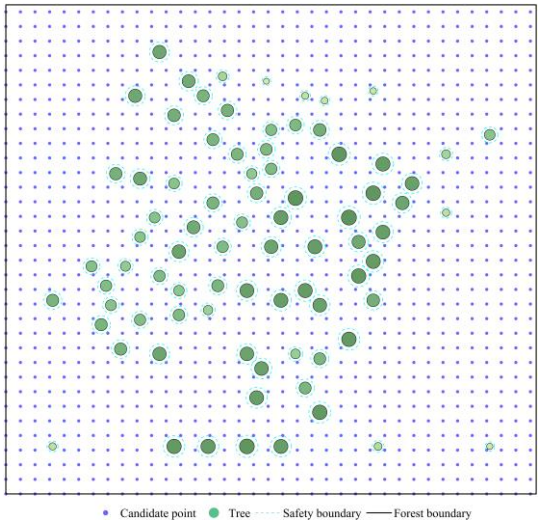

Figure 2. Two-dimensional forest environment and effective candidate scanning positions generation.

2.2 Visibility Analysis Based on Geometric Constraints

2.2.1 Recognition of Occlusion Situations

After reconstructing the forest vegetation spatial structure and generating candidate observation points, a quantitative visibility analysis is conducted to identify station combinations with high observational efficiency. The core of the visibility analysis lies in characterizing the occlusion relationships between the terrestrial laser scanner and individual target trees, that is, determining whether a target tree lies within the scanner’s field of view and whether it is occluded by other, closer trees, as well as quantifying the degree of occlusion. The analysis begins with the identification of the visible region of each individual tree. Each tree is simplified as a circle defined by its center $O(O_x, O_y)$ and radius r_1, as illustrated in Figure. 3. Taking a TLS observation point $M(M_x, M_y)$ as the viewpoint, an auxiliary radius R is introduced to compute the coordinates of the tangent points, where R is defined as half of the distance between the scanner and the circle center O. From the observation point M, two external tangent lines are drawn to the target circle on both sides, thereby determining the corresponding tangent points T_1 and T_2. The red arc segment between T_1 and T_2 represents the identifiable region of the tree stem within the TLS field of view. The mathematical formulation of this process is given in equations (1):

$$\begin{cases} (x-O_x)^2+(y-O_y)^2=r_1^2 \\ (x-C_x)^2+(y-C_y)^2=R^2 \\ C_x=(O_x+M_x)/2 \\ C_y=(O_y+M_y)/2 \\ R=\dfrac{1}{2}\sqrt{(M_x-O_x)^2+(M_y-O_y)^2} \end{cases} \quad (1)$$

where x = the x-coordinate of the tangent point in a Cartesian coordinate system

y = the y-coordinate of the tangent point in a Cartesian coordinate system

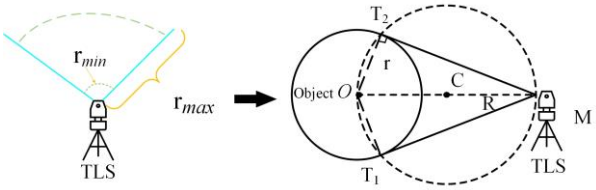

Figure 3. Illustration of the visibility analysis based on the tangent vector geometry between a point and a circle.

Based on the positional relationship between trees and the scanning positions, a polar coordinate system centered at each scanning position is established. The angular interval of each tree is then derived, representing the extent of its angular range under unobstructed conditions. By comparing the angular intervals among different trees, the occlusion relationships are subsequently determined. By comparing the angular intervals of different trees together with their distances to the observation point, occlusion relationships in the forest environment can be identified. These relationships are categorized into three types: (i) no occlusion, where the visible intervals of two trees do not overlap; (ii) partial occlusion, where the visible intervals partially overlap without complete coverage; and (iii) full occlusion, where the visible interval of the tree located behind is entirely covered by that of the tree in front. In the case of partial occlusion, the initially derived tangent points may be displaced due to overlapping angular intervals and therefore require correction, which can be formulated by solving the system of equations in equations (2):

$$\begin{cases} (x-O_{ocx})^2+(y-O_{ocy})^2=r^2 \\ \dfrac{x-O_{ocx}}{T_x-O_{ocx}}=\dfrac{y-O_{ocy}}{T_y-O_{ocy}} \\ argmin((I_x-O_{ocx})^2+(I_x-O_{ocy})^2) \end{cases} \quad (2)$$

where ocx = the x coordinates of the center of the partially occluded circle B

ocy = the y coordinates of the center of the partially occluded circle B

T_x = the x coordinates of a tangent point of circle A

T_y = the y coordinates of a tangent point of circle A

I_x = the x coordinates of the intersection point

I_y = the y coordinates of the intersection point

2.2.2 Visibility Analysis in Forest Environments

In terrestrial laser scanning observations, the visibility of the scanner is jointly influenced by the spatial distribution of trees and occlusion effects. To quantitatively characterize the observation range of a single tree from a scanning station, this study simplifies the scanner to a two-dimensional planar observation point and describes tree visibility using polar angular intervals. By emitting rays from measurement stations and calculating their geometric interactions with the circular cross-sections of trees, the visible angular range of each tree is determined, thereby quantifying the visibility range of candidate scanning positions. Based on the results mentioned earlier, we perform visibility calculations for each candidate scanning positions, as shown in Figure 4(b), primarily relying on the parameters of the scanning device, as shown in Figure 4(a), including the distance S between the laser scanner and the measured object, the horizontal angle α, and the incidence angle θ.

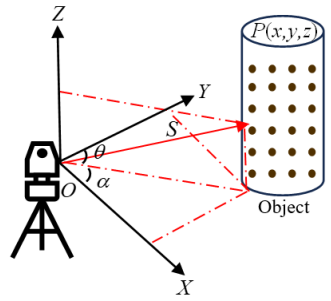

(a)

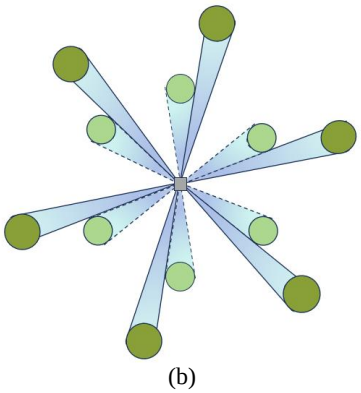

(b)

Figure 4. Illustration of scanner parameters. (a) TLS scanner parameters; (b) Analysis of visibility at scanning position.

For the quantitative description of the field of view characteristics of terrestrial laser scanners in forest stand environments. Let the coordinates of measurement station j be $S_j=(x_j,y_j)$, and the coordinates of the center of tree i be (x_i,y_i), with the radius corresponding to the breast height diameter denoted as r_i. The relative position vector and distance between the measurement station and the target tree can be expressed as:

$$\begin{cases} \overrightarrow{d_{ij}}=(x_i-x_j,y_i-y_j) \\ d_{ij}=\|\overrightarrow{d_{ij}}\| \end{cases} \quad (3)$$

According to two-dimensional geometric relationships, given the radius of the target tree crown, the azimuth θ_{ij} from the survey station to the center of the target tree, as well as the central angle a_{ij} of the tree visible from the survey station, can be expressed as:

$$\begin{cases} \theta_{ij}=\arctan(\dfrac{y_i-y_j}{x_i-x_j}) \\ \alpha_{ij}=\arcsin(\dfrac{r_i}{d_{ij}}) \end{cases} \quad (4)$$

Thus, the ideal visible angle range of tree i from measurement station S_j is:

$$I_{ij}=[\theta_{ij}-\alpha_{ij},\theta_{ij}+\alpha_{ij}] \quad (5)$$

This interval reflects the range of angles from the observation station within which the tree can be observed, with its length $2\alpha_{ij}$ representing the angular width of the tree within the scanner's field of view.

However, in forest scenarios, there exist complex occlusion relationships among trees. To simulate this occlusion, the present study addresses it through set difference operations on intervals of angles. If another tree k satisfies the following conditions:

$$d_{kj}<d_{ij}, I_{kj}\cap I_{ij}\neq\varnothing \quad (6)$$

In this case, the effective visible interval of Tree i needs to remove the occluded portion from the original interval:

$$I_{ij}^{*}=\left\{\theta\in I_{ij}\mid\forall k,(d_{kj}<d_{ij})\Rightarrow\theta\notin I_{kj}\right\} \quad (7)$$

The corrected angular range I_{ij}^{*} describes the truly visible portion of tree i from the perspective of station S_j, with the occlusion angles caused by foreground trees removed. This yields the actual visible part of the tree within the station's field of view, providing a foundation for subsequent multi-station integration and global coverage analysis.

In practical forest stand scanning, it is often necessary to set up scanners at multiple locations to reduce information loss caused

This contribution has been peer-reviewed. The double-blind peer-review was conducted on the basis of the full paper.
https://doi.org/10.5194/isprs-annals-XI-1-2026-111-2026 | © Author(s) 2026. CC BY 4.0 License.

by occlusions. If the same tree has partially visible intervals at different measurement stations, then the union of these angular intervals represents the overall visible range of the tree under the entire scanning system, referred to as the cumulative ring closure degree, or CDRC (Li. et al., 2021), as shown in Figure 5. When the circle is not scanned at all, the CDRC value is 0 °, and when the circle is fully scanned, the CDRC value is 360 °. The proposed CDRC metric quantifies the scanning completeness of each valid candidate for the optimal TLS scanning positions.

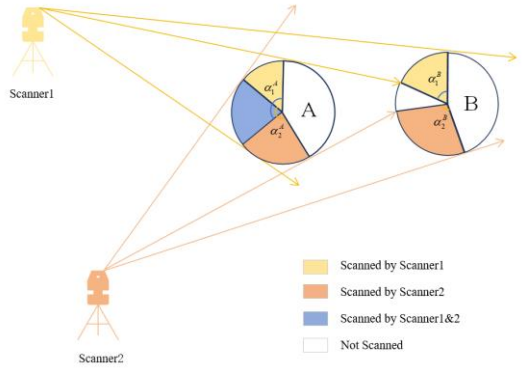

Figure 5. Illustration of the circular degree of ring closure for tree crowns with two scanners.

2.3 Hybrid Heuristic Integer Linear Programming Algorithm

To minimize the number of measurement stations while ensuring global coverage constraints, this study develops a two-stage optimization approach that combines heuristic search with Integer Linear Programming . This method first transforms the coverage optimization objective into a set cover problem: suppose the target area contains several occluded targets, and each candidate measurement station has angular visibility of some of the targets. The continuous angular visibility of each target is discretized into a finite set of angular segments after occlusion analysis. The constraints are transformed into the requirement that the cumulative number of visible angular segments for each target j exceeds the preset threshold τ, which is defined in this study as achieving at least 95% average angular coverage, that is, it satisfies:

$$\begin{cases} \sum_{i\in I}\sum_{k\in K} C_{ijk}x_i \geq \tau, \forall_j \in J \\ x_i \in \{0,1\}, \forall_i \in I \end{cases} \quad (8)$$

where $I=\{1,2,...,N\}$ = the set of candidate scanning positions

J = the set of target objects

K = the set of discrete angular segments

j = the target number, k represents the angular segment

C_{ijk} = the visibility of station i to target j within angular segment k

τ = the specified minimum visibility angle threshold

$x_i \in \{0,1\}$ = the candidate station i is selected

The entire objective function can thus be transformed into: $Z=\min\sum_{i\in I}x_i$, that is, under the premise of meeting the visual coverage requirements, the number of sites should be as small as possible.

Due to the complexity of scan planning and the observation network planning problem, this paper adopts a visibility-driven subproblem decomposition strategy. Firstly, visibility scores are constructed based on the cumulative visibility of candidate scanning positions to the targets, and retention ratios are set for both forest interior and exterior regions to form a dual-quota mechanism. Subsequently, a spatial minimum distance threshold is introduced to eliminate redundant points that are excessively clustered among high-scoring candidates, thereby enforcing spatial sparsity and controlling the size of the candidate set.

On this basis, a two-stage optimization is conducted by integrating heuristic algorithms with an integer linear programming model: in the heuristic stage, an initial set of measurement stations is constructed according to a greedy gain criterion to maximize the cumulative visible angles of uncovered targets. In the optimization stage, the sparse coverage matrix serves as the core constraint input, and the global optimal solution is obtained through ILP solving. Finally, a stepwise elimination process is carried out for post-processing, removing redundant stations that do not contribute to coverage completeness, resulting in an optimal and minimal measurement station configuration that satisfies coverage constraints.

3. Experimental Result and Analysis

3.1 Study Area and Parameter Settings

The forest plot data for this study were obtained from Lushan City, Jiangxi Province, China (N 29°33′4.37″, E 115°59′20.38″), as show in Figure 6. Cryptomeria was the dominant tree species in the sample plots. The UAV data were acquired using the ZENMUSE L2 LiDAR scanner. During the simulated terrestrial laser scanning process, the main parameter settings of the scanner and the experimental methods are shown in Table 1:

Scanner parameters	Value
The maximum measurement distance	130m
The minimum measurement distance	0.5m
Vertical field of view	280 °
Incident angle constraint	360 °
The grid resolution	1.5m
Number of candidate scanning positions	1775

Table 1. Parameter constraints of the laser scanning system's scanner

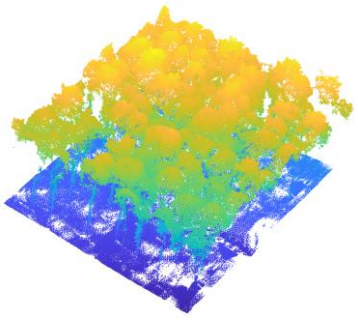

Figure 6. The research area.

3.2 Comparative Analysis of the Number of Sites

The hybrid heuristic integer programming optimization algorithm employed in this study achieves globally optimal visibility layout through a phased solution approach. The algorithm heuristically selects points based on visibility weighting to quickly identify an initial set of high-contribution sites. Subsequently, integer linear programming is used to perform a global optimization of the candidate results, thereby reducing redundant sites while satisfying minimum coverage constraints.

Based on the previously constructed safety buffer zone model and the vacant area identification method, this study generated a regular grid within the study area and systematically screened potential observation locations through multi-constraint visibility analysis, ultimately obtaining 1,775 candidate scanning positions that meet the visibility conditions. Experimental results indicate that the algorithm proposed in this study requires only seven candidate scanning positions to achieve complete coverage of the study area, with the findings illustrated in Figure 7.

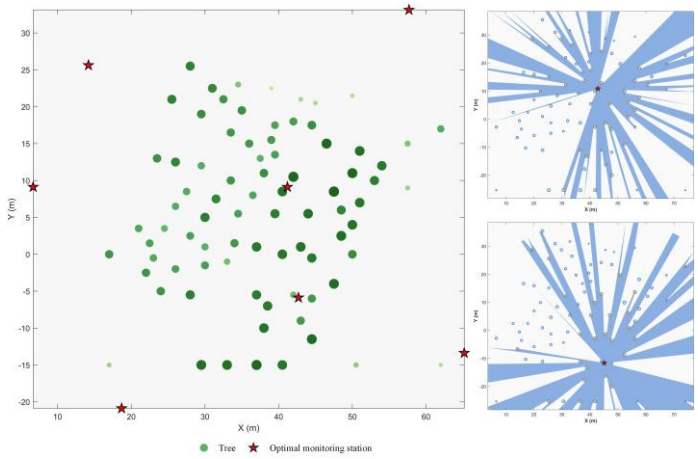

Figure 7. Results of the mixed heuristic integer linear programming algorithm at the station.

In terms of spatial distribution, the optimized measurement stations are evenly arranged across the forest area, enabling observations from multiple directions. At the forest boundaries, adjacent stations exhibit appropriate overlaps in their fields of view, effectively eliminating scanning blind spots. Within the interior regions, the stations maintain a high degree of field-of-view independence, thereby substantially reducing data redundancy caused by repeated observations. Overall, this layout achieves a favorable balance between coverage completeness and observational efficiency, indicating a well-optimized and practically efficient observation scheme.

To validate the performance of this method, this study conducted a comparative analysis with greedy algorithms (Figure 8a) and genetic algorithms (Figure 8b).

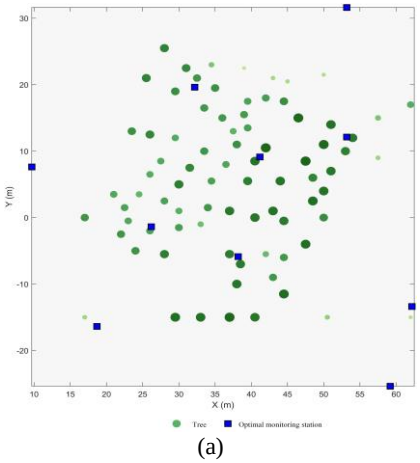

(a)

The results show that the greedy algorithm rapidly produces solutions by sequentially selecting survey stations with the largest marginal gain, leading to high computational efficiency. However, due to its inherently local search strategy, it is prone to suboptimal solutions under complex terrain and non-uniform visibility conditions, often resulting in an excessive number of survey stations and increased redundancy. Genetic algorithms, which rely on global search mechanisms, partially mitigate this limitation. Nevertheless, their performance is highly sensitive to parameter settings, and their computational cost increases sharply with the number of candidate scanning positions. In high-dimensional search spaces, they may further suffer from slow convergence and limited solution stability. In contrast, the proposed hybrid optimization method simultaneously optimizes both the number and spatial distribution of measurement stations while satisfying global coverage constraints. By balancing computational efficiency and solution stability, it demonstrates superior overall performance.

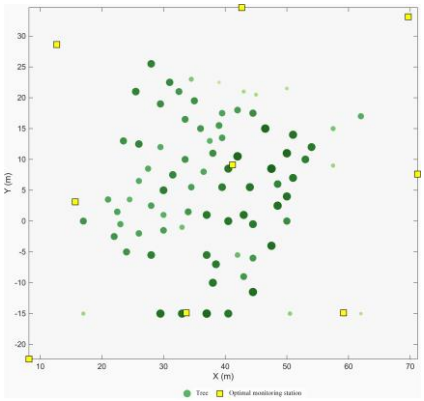

(b)

Figure 8. Experimental comparison results of different methods. (a) Experimental results of the greedy method; (b) Experimental results of the genetic method.

In contrast, the visibility-constrained optimization algorithm proposed in this paper achieves a higher level of integration between the search strategy and the constraint objectives. During the candidate scanning positions selection phase, the algorithm significantly reduces the search space through multi-scale field-of-view analysis and occlusion constraint filtering. During the optimization phase, it combines local visibility distribution with global coverage balance criteria, ensuring both the global optimality of the solution and improved convergence efficiency.

3.3 Coverage Comparison Analysis

Using the screened candidate scanning positions, local visibility computation and angular-domain occlusion analysis were conducted to model and evaluate the field-of-view characteristics at each observation location, resulting in a global scanning visibility distribution map for the study area. The statistical analysis shows that the average visible coverage of a single measurement station is 26.76%, indicating that in complex understory environments, the observational capability of an individual station is strongly constrained by forest structure and tree obstructions. Under multi-station joint observation, however, the visible areas of different stations effectively complement each other, increasing the overall coverage rate to 94.55% and achieving near-complete scanning coverage of the study area. The coverage results are illustrated in Figure. 9.

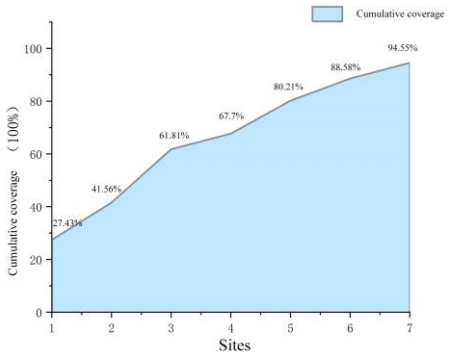

(a)

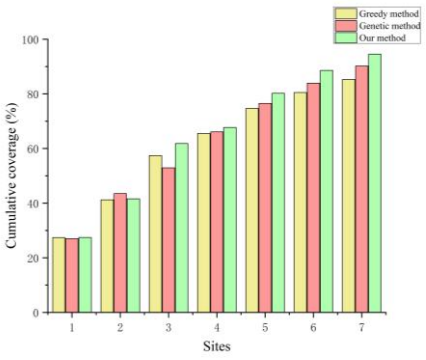

(b)

Figure 9. Coverage comparison. (a) Cumulative coverage of seven sites using this method; (b) Comparison of coverage among three methods.

To further validate the effectiveness and superiority of the proposed site layout optimization method, this study systematically conducted a quantitative comparison with the greedy algorithm and the genetic algorithm. From the perspective of cumulative coverage growth trends (Figure 9(a)), the proposed method achieved a regional coverage rate of 27.43% with the deployment of only the first monitoring station, demonstrating strong initial observation capability. As the number of stations gradually increased, the cumulative coverage rate exhibited a significant upward trend. Notably, after the deployment of the first four stations, the coverage rate had rapidly risen to 67.7%, reflecting the high marginal gains and effective spatial distribution of the initial station selections. Ultimately, upon the deployment of the seventh station, the total coverage rate reached 94.55%, achieving nearly complete observation of the study area.

Further horizontal comparison results are shown in Figure 9(b). It can be observed that in the initial stage with a smaller number of sites ($n \leqslant 3$), the greedy algorithm, by selecting the option with the maximum incremental gain at each step, demonstrates a relatively high initial coverage efficiency. However, as the number of sites increases, the local optimality characteristic of the algorithm gradually becomes evident. In comparison, genetic algorithms can maintain a certain level of global optimization capability in the middle and later stages. However, their convergence rate is relatively slow, and the stability of the solution is insufficient, resulting in limited improvement in coverage. If the goal is to achieve full global coverage, the greedy algorithm requires 10 observation stations, the genetic algorithm requires 9 stations, whereas the method proposed in this study achieves the same coverage with only 7 stations. Compared to the two benchmark algorithms, the number of stations is reduced by 30% and 22%, respectively, significantly enhancing station utilization and the spatial compactness of the observation network.

4. Conclusion

To address the limitations of UAV-LiDAR in capturing ground and understory structures due to canopy occlusion, this study introduces an intelligent terrestrial laser scanning station planning framework for air–ground cooperative observation. The proposed method employs a hybrid heuristic–integer linear programming strategy that first identifies high-contribution candidate regions through heuristic search to effectively reduce the solution space, and then applies ILP-based global optimization to ensure optimal coverage with minimal redundancy. This approach overcomes the local optimality issues of greedy algorithms and the slow convergence of genetic algorithms in large-scale discrete optimization.

This contribution has been peer-reviewed. The double-blind peer-review was conducted on the basis of the full paper.
https://doi.org/10.5194/isprs-annals-XI-1-2026-111-2026 | © Author(s) 2026. CC BY 4.0 License.

Experimental results demonstrate that the proposed method achieves 94.55% overall coverage with only seven TLS scanning positions, reducing the number of required stations by 30% and 22% compared to two benchmark algorithms. The results confirm that the optimized observation network is both spatially compact and computationally efficient, significantly enhancing the completeness and continuity of the integrated 3D point cloud.

Acknowledgements

This work was supported by the Outstanding Young Talents Funding of Jiangxi Province (20232ACB213017), Double Thousand Plan of Jiangxi Province (DHSQT42023002), Natural Science Foundation of Jiangxi Province (20242BAB25176, 20192BAB217010), National Natural Science Foundation of China (NSF) (42161060, 41801325) and Funding of National Key Laboratory of Uranium Resources Exploration-Mining and Nuclear Remote Sensing (2025QZ-YZZ-08, 2024QZ-TD-26) and for their financial support.

References

Ahn, J., Wohn, K., 2016. Interactive scan planning for heritage recording. *Multimed. Tools Appl.*, 75(7): 3655-3675.doi.org/10.1007/s11042-015-2473-0.

Calders, K., Adams, J., Armston, J., Bartholomeus, H., Bauwens, S., Bentley, L.P. et al., 2020. Terrestrial laser scanning in forest ecology: Expanding the horizon. *Remote Sens. Environ.*, 251: 112102. doi.org/10.1016/j.rse.2020.112102.

Chen, M., Koc, E., Shi, Z., Soibelman, L., 2018. Proactive 2D model-based scan planning for existing buildings. *Automat. Constr.*, 93: 165-177. doi.org/10.1016/j.autcon.2018.05.010.

Chen, Z., Zhang, W., Huang, R., Dong, Z., Chen, C., Jiang, L., Wang, H., 2022. 3D model-based terrestrial laser scanning (TLS) observation network planning for large-scale building facades. *Automat. Constr.*, 144: 104594. doi.org/10.1016/j.autcon.2022.104594.

Dehbi, Y., Leonhardt, J., Oehrlein, J., Haunert, J., 2021. Optimal scan planning with enforced network connectivity for the acquisition of three-dimensional indoor models. *Isprs J. Photogramm.*, 180: 103-116. doi.org/10.1016/j.isprsjprs.2021.07.013.

Latimer, E., Latimer, D., Saxena, R., C., Lyons, L., Michaux-Smith, L., Thayer, S., 2004, Sensor space planning with applications to construction environments, pp. 4454-4460 Vol.5. doi.org/ 10.1109/ROBOT.2004.1302419.

Hui, Z., He, Y., Jin, S., Chen, W., Cheng, P., Ziggah, Y.Y., 2025. Self-adaptive individual tree modeling based on skeleton graph optimization and fractal self-similarity. *Plant Phenomics*, 7(2): 100060. doi.org/10.1016/j.plaphe.2025.100060.

Bi, J., Yuan, H., Zhai, J., Zhou, M., Vincent Poor, H., 2022. Self-adaptive Bat Algorithm With Genetic Operations. *IEEE-CAA J. Automatic*, 9(7): 1284-1294. doi.org/10.1109/JAS.2022.105695.

Karaszewski, M., Adamczyk, M., Sitnik, R., 2016. Assessment of next-best-view algorithms performance with various 3D scanners and manipulator. *Isprs J. Photogramm.*, 119: 320-333. doi.org/10.1016/j.isprsjprs.2016.06.015.

Knechtel, J., Klingbeil, L., Haunert, J., Dehbi, Y., 2022. Optimal position and path planning for stop-and-go laserscanning for the acquisition of 3D building modes. *ISPRS Ann. Photogramm. Remote Sens. Spatial Inf. Sci.*, V-4-2022: 129-136. doi.org/10.5194/isprs-annals-V-4-2022-129-2022.

Li, L., Mu, X., Soma, M., Wan, P., Qi, J., Hu, R., Zhang, W., Tong, Y., Yan, G., 2021. An Iterative-Mode Scan Design of Terrestrial Laser Scanning in Forests for Minimizing Occlusion Effects. *Ieee T. Geosci. Remote*, 59(4): 3547-3566. doi.org/10.1109/TGRS.2020.3018643.

Liu, J., Liang, X., Hyyppä, J., Yu, X., Lehtomäki, M., Pyörälä, J., Zhu, L., Wang, Y., Chen, R., 2017. Automated matching of multiple terrestrial laser scans for stem mapping without the use of artificial references. *Int. J. Appl. Earth Obs.*, 56: 13-23. doi.org/10.1016/j.jag.2016.11.003.

Noichl, F., Stuecke, M., Thielen, C., Borrmann, A., 2024. Assessing and Improving Automated Viewpoint Planning for Static Laser Scanning Using Optimization Methods. *ISPRS Ann. Photogramm. Remote Sens. Spatial Inf. Sci.*, X-1-2024: 177-182. doi.org/10.5194/isprs-annals-X-1-2024-177-2024.

Panagiotidis, D., Abdollahnejad, A., Slavík, M., 2022. 3D point cloud fusion from UAV and TLS to assess temperate managed forest structures. *Int. J. Appl. Earth Obs.*, 112: 102917.doi.org/10.1016/j.jag.2022.102917.

Rebolj, D., Pučko, Z., Babič, N.., Bizjak, M., Mongus, D., 2017. Point cloud quality requirements for Scan-vs-BIM based automated construction progress monitoring. *Automat. Constr.*, 84: 323-334. doi.org/10.1016/j.autcon.2017.09.021.

Wujanz, D., Burger, M., Mettenleiter, M., Neitzel, F., 2017. An intensity-based stochastic model for terrestrial laser scanners. *Isprs J. Photogramm.*, 125: 146-155. doi.org/10.1016/j.isprsjprs.2016.12.006.